Measurement of Charged and Neutral Current e^-p Deep Inelastic Scattering Cross Sections at High Q^2

M. Derrick,[1] D. Krakauer,[1] S. Magill,[1] D. Mikunas,[1] B. Musgrave,[1] J. Repond,[1] R. Stanek,[1] R. L. Talaga,[1] H. Zhang,[1] R. Ayad,[2] G. Bari,[2] M. Basile,[2] L. Bellagamba,[2] D. Boscherini,[2] A. Bruni,[2] G. Bruni,[2] P. Bruni,[2] G. Cara Romeo,[2] G. Castellini,[2] M. Chiarini,[2] L. Cifarelli,[2] F. Cindolo,[2] A. Contin,[2] M. Corradi,[2] I. Gialas,[2] P. Giusti,[2] G. Iacobucci,[2] G. Laurenti,[2] G. Levi,[2] A. Margotti,[2] T. Massam,[2] R. Nania,[2] C. Nemoz,[2] F. Palmonari,[2] A. Polini,[2] G. Sartorelli,[2] R. Timellini,[2] Y. Zamora Garcia,[2] A. Zichichi,[2] A. Bargende,[3] J. Crittenden,[3] K. Desch,[3] B. Diekmann,[3] T. Doeker,[3] M. Eckert,[3] L. Feld,[3] A. Frey,[3] M. Geerts,[3] G. Geitz,[3] M. Grothe,[3] T. Haas,[3] H. Hartmann,[3] D. Haun,[3] K. Heinloth,[3] E. Hilger,[3] H.-P. Jakob,[3] U. F. Katz,[3] S. M. Mari,[3] A. Mass,[3] S. Mengel,[3] J. Mollen,[3] E. Paul,[3] Ch. Rembser,[3] R. Schattevoy,[3] D. Schramm,[3] J. Stamm,[3] R. Wedemeyer,[3] S. Campbell-Robson,[4] A. Cassidy,[4] N. Dyce,[4] B. Foster,[4] S. George,[4] R. Gilmore,[4] G. P. Heath,[4] H. F. Heath,[4] T. J. Llewellyn,[4] C. J. S. Morgado,[4] D. J. P. Norman,[4] J. A. O'Mara,[4] R. J. Tapper,[4] S. S. Wilson,[4] R. Yoshida,[4] R. R. Rau,[5] M. Arneodo,[6] L. Iannotti,[6] M. Schioppa,[6] G. Susinno,[6] A. Bernstein,[7] A. Caldwell,[7] N. Cartiglia,[7] J. A. Parsons,[7] S. Ritz,[7] F. Sciulli,[7] P. B. Straub,[7] L. Wai,[7] S. Yang,[7] Q. Zhu,[7] P. Borzemski,[8] J. Chwastowski,[8] A. Eskreys,[8] K. Piotrzkowski,[8] M. Zachara,[8] L. Zawiejski,[8] L. Adamczyk,[9] B. Bednarek,[9] K. Jeleń,[9] D. Kisielewska,[9] T. Kowalski,[9] E. Rulikowska-Zarębska,[9] L. Suszycki,[9] J. Zając,[9] A. Kotański,[10] M. Przybycień,[10] L. A. T. Bauerdick,[11] U. Behrens,[11] H. Beier,[11] J. K. Bienlein,[11] C. Coldewey,[11] O. Deppe,[11] K. Desler,[11] G. Drews,[11] M. Flasiński,[11] D. J. Gilkinson,[11] C. Glasman,[11] P. Göttlicher,[11] J. Grosse-Knetter,[11] B. Gutjahr,[11] W. Hain,[11] D. Hasell,[11] H. Hessling,[11] H. Hultschig,[11] Y. Iga,[11] P. Joos,[11] M. Kasemann,[11] R. Klanner,[11] W. Koch,[11] L. Köpke,[11] U. Kötz,[11] H. Kowalski,[11] J. Labs,[11] A. Ladage,[11] B. Löhr,[11] M. Löwe,[11] D. Lüke,[11] O. Mańczak,[11] J. S. T. Ng,[11] S. Nickel,[11] D. Notz,[11] K. Ohrenberg,[11] M. Roco,[11] M. Rohde,[11] J. Roldán,[11] U. Schneekloth,[11] W. Schulz,[11] F. Selonke,[11] E. Stiliaris,[11] B. Surrow,[11] T. Voss,[11] D. Westphal,[11] G. Wolf,[11] C. Youngman,[11] J. F. Zhou,[11] H. J. Grabosch,[12] A. Kharchilava,[12] A. Leich,[12] M. Mattingly,[12] A. Meyer,[12] S. Schlenstedt,[12] N. Wulff,[12] G. Barbagli,[13] P. Pelfer,[13] G. Anzivino,[14] G. Maccarrone,[14] S. De Pasquale,[14] L. Votano,[14] A. Bamberger,[15] S. Eisenhardt,[15] A. Freidhof,[15] S. Söldner-Rembold,[15] J. Schroeder,[15] T. Trefzger,[15] N. H. Brook,[16] P. J. Bussey,[16] A. T. Doyle,[16] J. I. Fleck,[16] D. H. Saxon,[16] M. L. Utley,[16] A. S. Wilson,[16] A. Dannemann,[17] U. Holm,[17] D. Horstmann,[17] T. Neumann,[17] R. Sinkus,[17] K. Wick,[17] E. Badura,[18] B. D. Burow,[18] L. Hagge,[18] E. Lohrmann,[18] J. Mainusch,[18] J. Milewski,[18] M. Nakahata,[18] N. Pavel,[18] G. Poelz,[18] W. Schott,[18] F. Zetsche,[18] T. C. Bacon,[19] I. Butterworth,[19] E. Gallo,[19] V. L. Harris,[19] B. Y. H. Hung,[19] K. R. Long,[19] D. B. Miller,[19] P. P. O. Morawitz,[19] A. Prinias,[19] J. K. Sedgbeer,[19] A. F. Whitfield,[19] U. Mallik,[20] E. McCliment,[20] M. Z. Wang,[20] S. M. Wang,[20] J. T. Wu,[20] Y. Zhang,[20] P. Cloth,[21] D. Filges,[21] S. H. An,[22] S. M. Hong,[22] S. W. Nam,[22] S. K. Park,[22] M. H. Suh,[22] S. H. Yon,[22] R. Imlay,[23] S. Kartik,[23] H.-J. Kim,[23] R. R. McNeil,[23] W. Metcalf,[23] V. K. Nadendla,[23] F. Barreiro,[24] G. Cases,[24] R. Graciani,[24] J. M. Hernández,[24] L. Hervás,[24] L. Labarga,[24] J. del Peso,[24] J. Puga,[24] J. Terron,[24] J. F. de Trocóniz,[24] G. R. Smith,[25] F. Corriveau,[26] D. S. Hanna,[26] J. Hartmann,[26] L. W. Hung,[26] J. N. Lim,[26] C. G. Matthews,[26] P. M. Patel,[26] L. E. Sinclair,[26] D. G. Stairs,[26] M. St. Laurent,[26] R. Ullmann,[26] G. Zacek,[26] V. Bashkirov,[27] B. A. Dolgoshein,[27] A. Stifutkin,[27] G. L. Bashindzhagyan,[28] P. F. Ermolov,[28] L. K. Gladilin,[28] Y. A. Golubkov,[28] V. D. Kobrin,[28] V. A. Kuzmin,[28] A. S. Proskuryakov,[28] A. A. Savin,[28] L. M. Shcheglova,[28] A. N. Solomin,[28] N. P. Zotov,[28] M. Botje,[29] F. Chlebana,[29] A. Dake,[29] J. Engelen,[29] M. de Kamps,[29] P. Kooijman,[29] A. Kruse,[29] H. Tiecke,[29] W. Verkerke,[29] M. Vreeswijk,[29] L. Wiggers,[29] E. de Wolf,[29] R. van Woudenberg,[29] D. Acosta,[30] B. Bylsma,[30] L. S. Durkin,[30] K. Honscheid,[30] C. Li,[30] T. Y. Ling,[30] K. W. McLean,[30] W. N. Murray,[30] I. H. Park,[30] T. A. Romanowski,[30] R. Seidlein,[30] D. S. Bailey,[31] G. A. Blair,[31] A. Byrne,[31] R. J. Cashmore,[31] A. M. Cooper-Sarkar,[31] D. Daniels,[31] R. C. E. Devenish,[31] N. Harnew,[31] M. Lancaster,[31] P. E. Luffman,[31] L. Lindemann,[31] J. D. McFall,[31] C. Nath,[31] V. A. Noyes,[31] A. Quadt,[31] H. Uijterwaal,[31] R. Walczak,[31] F. F. Wilson,[31] T. Yip,[31] G. Abbiendi,[32] A. Bertolin,[32] R. Brugnera,[32] R. Carlin,[32] F. Dal Corso,[32] M. De Giorgi,[32] U. Dosselli,[32] S. Limentani,[32] M. Morandin,[32] M. Posocco,[32] L. Stanco,[32] R. Stroili,[32] C. Voci,[32] J. Bulmahn,[33] J. M. Butterworth,[33] R. G. Feild,[33] B. Y. Oh,[33] J. J. Whitmore,[33] G. D'Agostini,[34] G. Marini,[34] A. Nigro,[34] E. Tassi,[34] J. C. Hart,[35] N. A. McCubbin,[35] K. Prytz,[35] T. P. Shah,[35] T. L. Short,[35] E. Barberis,[36] T. Dubbs,[36] C. Heusch,[36] M. Van Hook,[36] B. Hubbard,[36] W. Lockman,[36] J. T. Rahn,[36] H. F.-W. Sadrozinski,[36] A. Seiden,[36] J. Biltzinger,[37] O. Schwarzer,[37] R. J. Seifert,[37] A. H. Walenta,[37] G. Zech,[37] H. Abramowicz,[38] G. Briskin,[38] S. Dagan,[38] A. Levy,[38] T. Hasegawa,[39] M. Hazumi,[39] T. Ishii,[39] M. Kuze,[39] S. Mine,[39] Y. Nagasawa,[39] M. Nakao,[39] I. Suzuki,[39] K. Tokushuku,[39] S. Yamada,[39] Y. Yamazaki,[39] M. Chiba,[40] R. Hamatsu,[40] T. Hirose,[40] K. Homma,[40] S. Kitamura,[40] Y. Nakamitsu,[40] K. Yamauchi,[40] R. Cirio,[41] M. Costa,[41] M. I. Ferrero,[41] L. Lamberti,[41] S. Maselli,[41] C. Peroni,[41] R. Sacchi,[41] A. Solano,[41] A. Staiano,[41] M. Dardo,[42] D. C. Bailey,[43] D. Bandyopadhyay,[43] F. Benard,[43] M. Brkic,[43] M. B. Crombie,[43] D. M. Gingrich,[43] G. F. Hartner,[43] K. K. Joo,[43] G. M. Levman,[43] J. F. Martin,[43] R. S. Orr,[43] C. R. Sampson,[43]

 0031-9007/95/75(6)/1006(6)$06.00

R. J. Teuscher,[43] C. D. Catterall,[44] T. W. Jones,[44] P. B. Kaziewicz,[44] J. B. Lane,[44] R. L. Saunders,[44] J. Shulman,[44] K. Blankenship,[45] J. Kochocki,[45] B. Lu,[45] L. W. Mo,[45] W. Bogusz,[46] K. Charchuła,[46] J. Ciborowski,[46] J. Gajewski,[46] G. Grzelak,[46] M. Kasprzak,[46] M. Krzyżanowski,[46] K. Muchorowski,[46] R. J. Nowak,[46] J. M. Pawlak,[46] T. Tymieniecka,[46] A. K. Wróblewski,[46] J. A. Zakrzewski,[46] A. F. Żarnecki,[46] M. Adamus,[47] Y. Eisenberg,[48] U. Karshon,[48] D. Revel,[48] D. Zer-Zion,[48] I. Ali,[49] W. F. Badgett,[49] B. Behrens,[49] S. Dasu,[49] C. Fordham,[49] C. Foudas,[49] A. Goussiou,[49] R. J. Loveless,[49] D. D. Reeder,[49] S. Silverstein,[49] W. H. Smith,[49] A. Vaiciulis,[49] M. Wodarczyk,[49] T. Tsurugai,[50] S. Bhadra,[51] M. L. Cardy,[51] C.-P. Fagerstroem,[51] W. R. Frisken,[51] K. M. Furutani,[51] M. Khakzad,[51] and W.B. Schmidke[51]

(ZEUS Collaboration)

[1]*Argonne National Laboratory, Argonne, Illinois 60439*
[2]*University and INFN Bologna, Bologna, Italy*
[3]*Physikalisches Institut der Universität Bonn, Bonn, Federal Republic of Germany*
[4]*H.H. Wills Physics Laboratory, University of Bristol, Bristol, United Kingdom*
[5]*Brookhaven National Laboratory, Upton, New York 11973*
[6]*Calabria University, Physics Department and INFN, Cosenza, Italy*
[7]*Columbia University, Nevis Laboratory, Irvington on Hudson, New York 10533*
[8]*Institute of Nuclear Physics, Cracow, Poland*
[9]*Faculty of Physics and Nuclear Techniques, Academy of Mining and Metallurgy, Cracow, Poland*
[10]*Department of Physics, Jagellonian University, Cracow, Poland*
[11]*Deutsches Elektronen-Synchrotron DESY, Hamburg, Federal Republic of Germany*
[12]*DESY-Zeuthen, Institut für Hochenergiephysik, Zeuthen, Federal Republic of Germany*
[13]*University and INFN, Florence, Italy*
[14]*INFN, Laboratori Nazionali di Frascati, Frascati, Italy*
[15]*Fakultät für Physik der Universität Freiburg i.Br., Freiburg i.Br., Federal Republic of Germany*
[16]*Department of Physics and Astronomy, University of Glasgow, Glasgow, United Kingdom*
[17]*Hamburg University, I. Institute of Experimental Physics, Hamburg, Federal Republic of Germany*
[18]*Hamburg University, II. Institute of Experimental Physics, Hamburg, Federal Republic of Germany*
[19]*High Energy Nuclear Physics Group, Imperial College London, London, United Kingdom*
[20]*Physics and Astronomy Department, University of Iowa, Iowa City, Iowa 52242*
[21]*Institut für Kernphysik, Forschungszentrum Jülich, Jülich, Federal Republic of Germany*
[22]*Korea University, Seoul, Korea*
[23]*Department of Physics and Astronomy, Louisiana State University, Baton Rouge, Louisiana 70803*
[24]*Depto de Física Teóríca, Universidad Autónoma Madrid, Madrid, Spain*
[25]*Department of Physics, University of Manitoba, Winnipeg, Manitoba, Canada*
[26]*Department of Physics, McGill University, Montréal, Québec, Canada*
[27]*Moscow Engineering Physics Institute, Mosocw, Russia*
[28]*Moscow State University, Institute of Nuclear Physics, Moscow, Russia*
[29]*NIKHEF and University of Amsterdam, Amsterdam, The Netherlands*
[30]*Physics Department, The Ohio State University, Columbus, Ohio 43210*
[31]*Department of Physics, University of Oxford, Oxford, United Kingdom*
[32]*Dipartimento di Fisica dell' Universita and INFN, Padova, Italy*
[33]*Department of Physics, Pennsylvania State University, University Park, Pennsylvania 16802*
[34]*Dipartimento di Fisica, Univ. 'La Sapienza' and INFN, Rome, Italy*
[35]*Rutherford Appleton Laboratory, Chilton, Didcot, Oxon, United Kingdom*
[36]*University of California, Santa Cruz, California 95064*
[37]*Fachbereich Physik der Universität-Gesamthochschule Siegen, Federal Republic of Germany*
[38]*School of Physics, Tel-Aviv University, Tel Aviv, Israel*
[39]*Institute for Nuclear Study, University of Tokyo, Tokyo, Japan*
[40]*Department of Physics, Tokyo Metropolitan University, Tokyo, Japan*
[41]*Universita di Torino, Dipartimento di Fisica Sperimentale and INFN, Torino, Italy*
[42]*II Faculty of Sciences, Torino University and INFN, Alessandria, Italy*
[43]*Department of Physics, University of Toronto, Toronto, Ontario, Canada*
[44]*Physics and Astronomy Department, University College London, London, United Kingdom*
[45]*Physics Department, Virginia Polytechnic Institute and State University, Blacksburg, Virginia 24061*
[46]*Institute of Experimental Physics, Warsaw University, Warsaw, Poland*
[47]*Institute for Nuclear Studies, Warsaw, Poland*
[48]*Nuclear Physics Department, Weizmann Institute, Rehovot, Israel*
[49]*Department of Physics, University of Wisconsin, Madison, Wisconsin 53706*
[50]*Faculty of General Education, Meiji Gakuin University, Yokohama, Japan*
[51]*Department of Physics, York University, North York, Ontario, Canada*

(Received 31 March 1995)

Deep inelastic $e^- p$ scattering has been studied in both the charged current (CC) and neutral current (NC) reactions at momentum transfers squared Q^2 above 400 GeV^2 using the ZEUS detector at the HERA ep collider. The CC and NC total cross sections, the NC to CC cross section ratio, and the differential cross sections $d\sigma/dQ^2$ are presented. From the Q^2 dependence of the CC cross section, the mass term in the CC propagator is determined to be $M_W = 76 \pm 16 \pm 13$ GeV.

PACS numbers: 13.60.Hb, 12.15.Ji, 14.70.Fm

Lepton-nucleon scattering is an important technique for studying the constituents of the nucleon and their interactions. In the standard model [1], electron-proton (ep) scattering occurs via the exchange of gauge bosons (γ, Z^0, $W^\pm$). At long wavelengths (small momentum transfers), photon mediated interactions dominate over the exchange of the heavy gauge bosons. However, at the ep storage ring HERA, for the first time, scattering can be observed at sufficiently short wavelengths (large momentum transfers) that the "weak" and "electromagnetic" scattering amplitudes are comparable in magnitude.

The differential Born cross section for deep inelastic scattering (DIS) with unpolarized $e^- p$ beams can be expressed as [2]

$$\frac{d^2\sigma}{dx\,dQ^2} = \frac{2\pi\alpha^2}{xQ^4}[\{1 + (1 - y)^2\}\mathcal{F}_2 + \{1 - (1 - y)^2\}x\mathcal{F}_3],$$

where the $\mathcal{F}_i(x, Q^2)$ functions describe the proton structure and couplings. In this equation Q^2 is the negative square of the four-momentum transfer, y is the fractional energy transfer from the lepton in the proton rest frame, α is the electromagnetic fine-structure constant, and x is the proton momentum fraction carried by the struck parton. These variables are related by $Q^2 = sxy$, where $\sqrt{s}$ is the center-of-mass energy. The $\mathcal{F}_i$ can be expressed as sums over quark flavors f of the proton's quark densities $q_f(x, Q^2)$ weighted according to the gauge structure of the scattering amplitudes. For the neutral current (NC) reaction, $e^- p \to e^- X$, mediated by γ and Z^0 exchange, they can be written as

$$\mathcal{F}_2^{\mathrm{NC}} = \sum_f q_f^+[e_f^2 + 2v_e v_f e_f \mathcal{P}_Z + (v_e^2 + a_e^2)(v_f^2 + a_f^2)\mathcal{P}_Z^2],$$

$$x\mathcal{F}_3^{\mathrm{NC}} = \sum_f q_f^-[-2a_e a_f e_f \mathcal{P}_Z + 4v_e a_e v_f a_f \mathcal{P}_Z^2],$$

where $q_f^\mp = \{xq_f(x, Q^2) \pm x\bar{q}_f(x, Q^2)\}$, a_e and v_e are the axial and vector couplings of the e^- to the Z^0, and a_f and v_f are the analogous couplings for a quark of flavor f, which has electric charge e_f [1]. $\mathcal{P}_Z$ is the ratio of Z^0-to-photon propagators, given by $\mathcal{P}_Z = Q^2/(Q^2 + M_Z^2)$, where M_Z is the mass of the Z boson.

For charged current (CC) scattering, $e^- p \to \nu_e X$, in which a W boson with mass M_W is exchanged, the functions are

$$\mathcal{F}_2^{\mathrm{CC}} = \frac{x\mathcal{P}_W^2}{8\sin^4\theta_W}\sum_{k,m}[|V_{km}|^2 u_k + |V_{mk}|^2 \bar{d}_m],$$

$$x\mathcal{F}_3^{\mathrm{CC}} = \frac{x\mathcal{P}_W^2}{8\sin^4\theta_W}\sum_{k,m}[|V_{km}|^2 u_k - |V_{mk}|^2 \bar{d}_m],$$

where k and m are the generation indices of up-type quarks $u_k(x, Q^2)$ and down-type antiquarks $\bar{d}_m(x, Q^2)$, V is the Cabibbo-Kobayashi-Maskawa quark mixing matrix, θ_W is the weak mixing angle, and $\mathcal{P}_W = Q^2/(Q^2 + M_W^2)$. At lowest order, $G_F M_W^2 = \pi\alpha/\sqrt{2}\sin^2\theta_W$, where G_F is the Fermi constant.

In 1993, HERA collided 26.7 GeV e^- with 820 GeV p, giving $\sqrt{s} = 296$ GeV. At this high center-of-mass energy, DIS can be investigated at much higher Q^2 than in fixed target experiments. The predicted DIS cross sections at fixed x over a large Q^2 range depend both on the electroweak theory for the propagators and couplings and on quantum chromodynamics (QCD) for the parton density evolution. The structure functions $\mathcal{F}_2$ have been measured [3] in ep and μp scattering for Q^2 up to $\sim$5 (150) GeV^2 at $x = 0.03$ (0.3). The parton density distributions [4,5] inferred from those measurements were extrapolated to our Q^2 region using the next-to-leading-order QCD evolution equations [6]. At x of 0.03 (0.3), the up-quark density is predicted to change by 21% (-39%) as Q^2 increases from 5 to 16 000 GeV^2. The NC propagator varies by 7 orders of magnitude over the same Q^2 interval.

This paper reports measurements of integrated and differential cross sections $d\sigma/dQ^2$ for NC and CC DIS with $Q^2 > 400$ GeV^2 using a luminosity of 0.540 ± 0.016 pb^{-1}. ZEUS [7] and H1 [8] have previously reported on NC DIS cross section measurements at lower Q^2. H1 has also measured the CC total cross section [9] and demonstrated that the CC propagator mass is finite.

In ZEUS [7], charged particles are tracked by drift chambers operating in an axial magnetic field of 1.43 T. The superconducting solenoid is surrounded by a compensating uranium-scintillator calorimeter (CAL) with an electromagnetic (hadronic) energy resolution of $18\%/\sqrt{E(\mathrm{GeV})}$ [$35\%/\sqrt{E(\mathrm{GeV})}$] and a subnanosecond time resolution. The CAL covers the polar angles between 2.2° and 176.5°, defined with respect to the incident proton direction. The CAL is segmented in depth into electromagnetic and hadronic sections, with a total thickness of 4 to 7 interaction lengths. Surrounding the CAL is an iron magnetic return yoke instrumented for muon detection. The luminosity is measured by the rate of high-energy photons from the reaction $ep \to ep\gamma$.

Data were collected with a three-level trigger. The first-level trigger was based on electromagnetic energy, transverse energy, and total energy deposits in the CAL [7]. The thresholds, between 2 and 15 GeV, were well below the off-line selection cuts. The second-level trigger rejected p-gas events (proton interactions with residual gas in the beam pipe upstream of the detector) recognized by CAL energy deposited earlier than the ep crossing. The third-level trigger selected events as NC DIS candidates if $E - P_z$ exceeded 25 GeV, where E and P_z are the total energy and z component of the momentum measured in the calorimeter. If no energy escapes through the rear beam hole, $E - P_z \approx 2E_e$, where E_e is the electron beam energy. Events were selected as CC DIS candidates if $\not{p}_t$, the absolute value of the missing transverse momentum measured by the calorimeter, exceeded 9 GeV, and there was either more than 10 GeV deposited in the forward part of the CAL or at least one track reconstructed in the drift chambers.

The acceptances and measurement resolutions for signal and background events were calculated using Monte Carlo methods. Simulated CC and NC DIS events, generated using LEPTO [10] interfaced to HERACLES [11] by DJANGO [12], were passed through a GEANT [13] based detector simulation, and subsequently analyzed with the same reconstruction and off-line selection procedures as the data. The efficiencies and acceptances were found to have negligible dependences on either the model of the hadronic final state [10,14] or the proton parton density parametrizations [4] used in the simulation.

As the ZEUS detector is nearly hermetic, it is possible to reconstruct the kinematic variables (x, y, Q^2) for NC DIS using different combinations of the angles and energies of the scattered lepton and hadronic systems [7]. Three reconstruction methods were relevant to this analysis. The electron (e) method uses E_e' and θ_e, the energy and polar angle of the scattered electron. The hadronic, or Jacquet-Blondel (JB) [15], method reconstructs y and Q^2 as $y_{\rm JB} = (E_h - P_{z,h})/2E_e$ and $Q^2_{\rm JB} = P^2_{t,h}/(1 - y_{\rm JB})$, where E_h, $P_{z,h}$, and $P_{t,h}$ are the energy, the z component of momentum, and the transverse momentum of the hadronic system. The double angle (DA) method uses θ_e and γ_h, the polar angle of the struck quark given by $\cos\gamma_h = [P^2_{t,h} - (2E_e y_{\rm JB})^2]/[P^2_{t,h} + (2E_e y_{\rm JB})^2]$. The DA method, which estimates Q^2 with small bias and good resolution, was used for NC events [7]. For CC DIS, the hadronic (JB) method was used.

The off-line NC DIS event selection required an electron candidate with $E_e' > 10$ GeV in the calorimeter and $E - P_z > 35$ GeV. To reject backgrounds from photoproduction events with a fake electron (mostly π^0's at small polar angles) the electron candidate was required to have a matching track and to satisfy $y_e < 0.95$. Cosmic-ray triggers were rejected by requiring $\not{p}_t/\sqrt{E_t} < 2\ \mathrm{GeV}^{1/2}$. A final cut required Q^2, as reconstructed by the DA and e methods, to be consistent: $0.7 < Q_e^2/Q^2_{\rm DA} < 1.2$. After these selections, 436 events with $Q^2_{\rm DA} > 400\ \mathrm{GeV}^2$ remained. The photoproduction background is less than 2%. More than 85% of all Monte Carlo NC DIS events with $Q^2 > 400\ \mathrm{GeV}^2$ pass all of the above cuts. The spectra of x and Q^2 for the data and the Monte Carlo simulation are shown in Figs. 1(a) and 1(b).

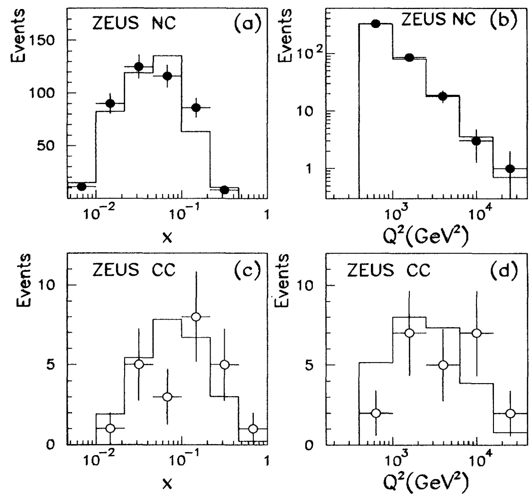

FIG. 1. (a) x for NC events, (b) Q^2 for NC events, (c) x for CC events, and (d) Q^2 for CC events. The points with error bars are ZEUS data. The histograms are the predicted numbers of events from the absolutely normalized simulation.

The NC DIS cross sections in five bins of Q^2 between 400 GeV ^{2} and the kinematic limit of 87 500 GeV ^{2} are given in Table I. The Born cross section was calculated for each bin as $\sigma_{\rm NC} = N_{\rm NC}\delta r_{\rm NC}/\mathcal{L}\,\mathcal{A}_{\rm NC}$. $N_{\rm NC}$ is the number of NC DIS events reconstructed in the bin, $\delta r_{\rm NC}$ is the radiative correction factor, and $\mathcal{L}$ is the luminosity. The acceptance for the bin, $\mathcal{A}_{\rm NC}$, was calculated from the NC DIS Monte Carlo event sample, as the ratio of the number of events which passed all cuts and were reconstructed in the Q^2 bin to the number of events with the true Q^2 in the bin. $\mathcal{A}_{\rm NC}$ varies between 0.79 and 0.85. HERACLES [11] was used to calculate $\delta r_{\rm NC}$, which was in the range 0.88 to 0.95, with an uncertainty of less than 4%.

The systematic errors on $\mathcal{A}_{\rm NC}$ include 4% due to the uncertainty of the calorimeter energy response, 3% for the efficiency of the calorimeter-track matching for the electron, 4% for the efficiency of the electron identification algorithm, and 5% in the lowest Q^2 bin for the efficiency of the $Q_e^2/Q^2_{\rm DA}$ cut.

CC DIS events are characterized by a large $\not{p}_t$ due to the final-state neutrino. The 36 000 CC triggers are mainly from upstream p-gas or cosmic-ray interactions. The off-line CC DIS selection required $\not{p}_t > 12$ GeV and a vertex, formed from two or more tracks, within 45 cm of the nominal interaction point. Events with more than 40 tracks not associated with the vertex were rejected. To reduce the remaining p-gas background, for which the reconstructed transverse energy was concentrated at small polar angles, events with $\not{p}_t^{\rm outer} < 0.7\not{p}_t$ were rejected, where $\not{p}_t^{\rm outer}$ is the missing transverse momentum in the calorimeter excluding the $1.0 \times 1.0\ \mathrm{m}^2$ region around the forward beam pipe. The 117 candidates remaining were mostly cosmic-ray events, including cosmic-ray muons coincident with a p-gas interaction. Single muons were

TABLE I. Events observed and integrated Born cross sections for NC and CC DIS. Errors shown are statistical, followed by systematic (including 3.5% luminosity uncertainty). The standard model cross sections $\sigma^{\rm SM}$ are calculated with LEPTO [10] using the MRSD$'_-$ parton distributions [4]. The predictions for an infinite mass in the CC propagator $\sigma_{\rm CC}^{\infty}$ are shown. In the last three rows the NC and CC total cross sections and their ratios are given for $Q^2 > Q^2_{\rm min}$.

$Q^2_{\rm min}$ (GeV^2)	400	1000	2500	6250	15625
$Q^2_{\rm max}$ (GeV^2)	1000	2500	6250	15625	87500
$N_{\rm NC}$	328	86	18	3	1
$\sigma_{\rm NC}$ (pb)	629	163	36	5.8	2.0
$\delta\sigma_{\rm NC}$ (pb)	$\pm 38 \pm 73$	$\pm 18 \pm 16$	$\pm 9 \pm 4$	$^{+3.6}_{-3.2} \pm 0.6$	$^{+2.9}_{-1.6} \pm 0.3$
$\sigma^{\rm SM}_{\rm NC}$ (pb)	644	167	41	8.8	1.1
$N_{\rm CC}$	2	7	5	7	2
$\sigma_{\rm CC}$ (pb)	5.8	16.8	12.3	16.8	3.4
$\delta\sigma_{\rm CC}$ (pb)	$^{+4.6}_{-3.8} \pm 0.9$	$^{+6.7}_{-6.1} \pm 2.3$	$^{+5.8}_{-5.3} \pm 1.7$	$^{+6.7}_{-6.1} \pm 2.2$	$^{+2.7}_{-2.1} \pm 0.4$
$\sigma^{\rm SM}_{\rm CC}$ (pb)	13.3	17.1	15.9	8.0	1.6
$\sigma^{\infty}_{\rm CC}$ (pb)	17.5	28.3	41.8	46.0	21.2
			Cross sections for $Q^2 > Q^2_{\rm min}$		
$\sigma_{\rm NC}$ (pb)	837 ± 100	209 ± 27	46 ± 12	8.0 ± 4.1	2.0 ± 1.7
$\sigma_{\rm CC}$ (pb)	57 ± 20	50 ± 13	34 ± 10	21 ± 3.1	3.4 ± 2.7
$\sigma_{\rm NC}/\sigma_{\rm CC}$	$14.7^{+3.4}_{-3.2}$	$4.2^{+1.3}_{-0.9}$	$1.4^{+0.6}_{-0.4}$	$0.4^{+0.3}_{-0.1}$	$0.7^{+1.3}_{-0.6}$

rejected on the basis of their characteristic spatial distribution of energy deposition in the calorimeter or muon chambers. Additionally, the times of all energy deposits in the calorimeter were required to be consistent with an ep interaction.

The events passing all selection criteria were scanned, and one cosmic-ray event was removed, leaving 23 events with $Q^2 > 400$ GeV ^{2} in the final CC DIS sample. From Monte Carlo simulations, we expect fewer than one background event from photoproduction. Figures 1(c) and 1(d) show the reconstructed x and Q^2 distributions for the data sample with $Q^2 > 400$ GeV^2 compared to the Monte Carlo simulation for CC DIS.

The CC DIS Born cross sections, $\sigma_{\rm CC} = N_{\rm CC}\delta r_{\rm CC}/\mathcal{L}\mathcal{A}_{\rm CC}$, are shown in Table I. The acceptances $\mathcal{A}_{\rm CC}$ are in the range 0.67–0.80, except for the bin at largest Q^2, where it is 1.10. 75% of the Monte Carlo CC DIS events generated with $Q^2 > 400$ GeV ^{2} pass all selection cuts. The radiative correction factors $\delta r_{\rm CC}$ are in the range 1.02–1.03. The systematic errors on $\mathcal{A}_{\rm CC}$ include 5% due to the dependence on the $\not{p}_t$ and the $\not{p}_t^{\rm outer}/\not{p}_t$ thresholds, 5% for the efficiency to reconstruct a vertex, 8% in the lowest Q^2 bin due to the calorimeter energy scale, and 9% (20%) on the lower four bins (highest Q^2 bin) due to the hadronic energy reconstruction.

The differential Born cross sections $d\sigma/dQ^2$ for both NC and CC scattering, shown in Fig. 2, agree with the standard model predictions. The ratios of the NC to CC total cross sections for $Q^2 > Q^2_{\rm min}$ are listed in Table I. From the lowest bin in Q^2 to the highest, the ratio of $d\sigma_{\rm NC}/dQ^2$ to $d\sigma_{\rm CC}/dQ^2$ decreases by 2 orders of magnitude to around unity, thus demonstrating the equal strengths of the weak and electromagnetic forces at high Q^2.

Because of the massless photon propagator, the NC cross section decreases rapidly with Q^2. The Q^2 dependence of the CC cross section depends on the mass M_W in the CC propagator. The CC cross sections expected in the limit of infinite propagator mass, $\sigma^{\infty}_{\rm CC}$, are inconsistent with the data, as shown in Table I. Fitting $d\sigma_{\rm CC}/dQ^2$ with M_W as the free parameter, and G_F fixed, we find $M_W = 76 \pm 16({\rm stat}) \pm 13({\rm syst})$ GeV, which agrees with the $W^\pm$ mass, $M_W = 80.22 \pm 0.26$ GeV [1], measured at hadron colliders.

We express our deep gratitude to the people from DESY and outside institutes whose dedicated efforts made possible the successful operation of the ZEUS experiment. The inventiveness of the HERA machine group is appreciated. We thank the DESY directorate for strong support and encouragement. This work was supported by the Natural Sciences and Engineering Research Council of

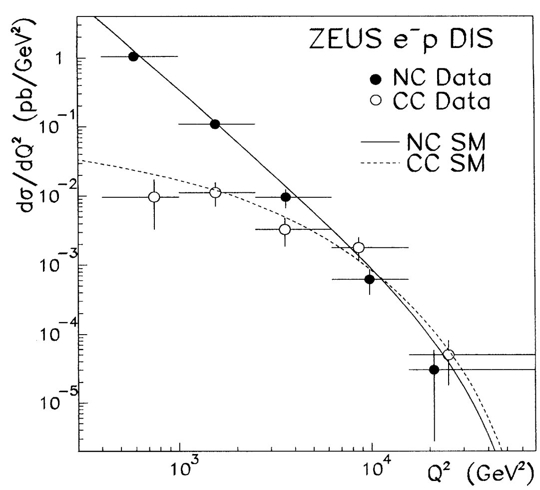

FIG. 2. $d\sigma/dQ^2$ for CC and NC DIS. The points with errors are the data, and the curves are the standard model Born cross sections. The data are plotted at the average Q^2 of the events in each bin.

Canada, FCAR of Québec, German Federal Ministry for Research and Technology (BMFT), Volkswagen Foundation, MINERVA Gesellschaft für Forschung, Israeli Academy of Science, German Israeli Foundation, Italian National Institute for Nuclear Physics (INFN), Japanese Ministry of Education, Science and Culture, Korean Ministry of Science and Korea Science and Engineering Foundation, Netherlands Foundation for Research on Matter, Polish State Committee for Scientific Research, Foundation for Polish-German Collaboration, Deutsche Forschungsgemeinschaft (DFG), Spanish Ministry of Education and Science, U.K. Particle Physics and Astronomy Research Council (PPARC), U.S. Department of Energy (DOE), and U.S. National Science Foundation (NSF).

[1] For a concise summary of the standard model, see Particle Data Group, L. Montanet *et al.,* Phys. Rev. D **50**, 1304 (1994).

[2] G. Ingelman and R. Rückl, Phys. Lett. B **201**, 369 (1988).

[3] J. Feltesse, Report No. DAPNIA/SPP 94-35.

[4] A. D. Martin, W. J. Stirling, and R. G. Roberts, Phys. Lett. B **306**, 145 (1993).

[5] CTEQ Collaboration, H. L. Lai *et al.,* Michigan State University Report No. MSU-HEP-41024, October 1994; M. Glück, E. Reya, and A. Vogt, Phys. Lett. B **306**, 391 (1993).

[6] V. Gribov and L. Lipatov, Sov. J. Nucl. Phys. **15**, 438 (1972); G. Altarelli and G. Parisi, Nucl. Phys. **B126**, 298 (1977).

[7] ZEUS Collaboration, M. Derrick *et al.,* Z. Phys. C **65**, 379 (1995).

[8] H1 Collaboration, I. Abt *et al.,* Report No. DESY 95-006.

[9] H1 Collaboration, I. Abt *et al.,* Phys. Lett. B **324**, 241 (1994).

[10] LEPTO 6.1 with the matrix element plus parton shower option, see G. Ingelman, in *Proceedings of the Workshop on Physics at HERA,* edited by W. Buchmüller and G. Ingelman (DESY, Hamburg, 1992), Vol. 3, p. 1366.

[11] HERACLES 4.1: A. Kwiatkowski, H. Spiesberger, and H.-J. Möhring, in *Proceedings of the Workshop on Physics at HERA*, Ref. [10], Vol. 3, p. 1294.

[12] DJANGO 1.0: G. Schuler and H. Spiesberger, in *Proceeding of the Workshop on Physics at HERA*, Ref. [10], Vol. 3, p. 1419.

[13] GEANT 3.13: R. Brun *et al.,* CERN Report No. DD/EE-84-1, 1987.

[14] ARIADNE with the color dipole + boson gluon fusion model: L. Lönnblad, Comp. Phys. Commun. **71**, 15 (1992).

[15] F. Jacquet and A. Blondel, in Proceedings of the Study for an ep Facility in Europe 79/48, edited by U. Amaldi (1979), p. 391.